Microfluidic metamaterial sensor: Selective trapping and remote sensing of microparticles

Kailing Shih, Prakash Pitchappa, Manukumara Manjappa, Chong Pei Ho, Ranjan Singh, and Chengkuo Lee

Citation: J. Appl. Phys. **121**, 023102 (2017); doi: 10.1063/1.4973492
View online: http://dx.doi.org/10.1063/1.4973492
View Table of Contents: http://aip.scitation.org/toc/jap/121/2
Published by the American Institute of Physics

Microfluidic metamaterial sensor: Selective trapping and remote sensing of microparticles

Kailing Shih,[1,2,5] Prakash Pitchappa,[1,2] Manukumara Manjappa,[3,4] Chong Pei Ho,[1,2,5] Ranjan Singh,[3,4] and Chengkuo Lee[1,2,6,a)]

[1]*Department of Electrical and Computer Engineering, National University of Singapore, 117576 Singapore*
[2]*Center for Intelligent Sensors and MEMS (CISM), National University of Singapore, 117576 Singapore*
[3]*Division of Physics and Applied Physics, School of Physical and Mathematical Sciences, Nanyang Technological University, 637371 Singapore*
[4]*Center for Disruptive Photonic Technologies, The Photonics Institute, 50 Nanyang Avenue, Nanyang Technological University, 639798 Singapore*
[5]*Department of Micro/Nano Electronics, Shanghai Jiao Tong University, Dong Chuan Road 800, 200240 Shanghai, People's Republic of China*
[6]*Graduate School for Integrative Science and Engineering, National University of Singapore, Singapore*

(Received 2 November 2016; accepted 19 December 2016; published online 9 January 2017)

We experimentally demonstrate the integration of a microfluidic trap array on top of metamaterial resonators for size selective trapping and remote sensing of microparticles. A split-ring resonator (SRR) design supports strongly confined electric field in the capacitive split gap at the fundamental inductive-capacitive resonance mode. The tightly confined electric field in the SRR gap forms a hot-spot that has become an enabling platform for sensing applications. Here, we extend the concept of metamaterial sensing to "trapping and sensing" by fabricating trapezoidal shaped structures near the split gap that enables trapping of microparticles in the split-gap region of each SRR. The proposed *microfluidic metamaterial sensor* enables sensing of different refractive index microparticles in terms of change in the transmitted amplitude and resonance frequency of the fundamental resonance mode operating in the terahertz spectral region. The proposed approach exploits the advantages offered by microfluidics, metamaterials, and terahertz technologies to form an ideal platform for ultra-sensitive, label-free, remote, and non-destructive detection of micro-substances. *Published by AIP Publishing*. [http://dx.doi.org/10.1063/1.4973492]

I. INTRODUCTION

An electromagnetic metamaterial is a periodic array of sub-wavelength structures that can be engineered to achieve specific electromagnetic properties on demand.[1,2] This has led to the demonstration of numerous interesting electromagnetic properties such as negative refractive index,[3,4] perfect absorption,[5,6] sub-wavelength focusing,[7] and many more.[8–10] Interestingly, the properties of the metamaterials are strongly dependent on the geometry of their unit cell, and thereby passively and actively varying the size and shape of the unit cell, a precise control of the metamaterial properties can be readily achieved.[11–18] Alternatively, metamaterials are also explored as a sensing platform due to their strong response to the changes in the surrounding medium and strong enhancement of the field strengths at specific portions of the resonator geometry.[19] In particular, metamaterials operating in the THz spectral region are of great interest, due to their lower illumination energy and their unit cell dimensions matching the size of microscale particles and biological cells.[20–24]

Earlier reports have shown the sensing capabilities of the THz metamaterials by covering the entire surface of the metamaterial resonators with the material of interest for sensing.[25–33] Park *et al.*, have reported detection of microorganisms,[25–27] while on the other hand chemical and biomolecule sensing has also been explored.[28–33] However, these reports provide the qualitative estimations on the sensing of the thin film or biological samples in the form of their statistical average value. These techniques also require a relatively large volume of sensing medium due to the need for uniform coating.[34] Hence, to achieve more quantitative sensing of particles, the number of particles per resonator geometry and the location at which the particle is placed become extremely crucial. This can be realized by integrating microfluidic trapping structures onto metamaterial resonators operating in the THz spectral range. Integration of metamaterials and microfluidics has been demonstrated in the gigahertz (GHz) spectral range for liquid sensing.[35,36] Microfluidics enables the precise manipulation of fluid with a small volume inside a microchannel by utilizing the microelectromechanical system (MEMS) technology.[37–41] It also facilitates precise handling, sorting, and trapping of microsubstances suspended in liquid solution.[42–44] By proper design of the flow resistance, a single particle trapping can be positioned at the desired area of the microfluidic device.[45–48] Hence, by integrating microfluidic systems with metamaterials, it is possible to control the volume of the sample and the location of microsubstances without any chemical modification or additional handling. Moreover, the versatility of metamaterial resonator designs with the ease of microfluidic integration offers a new set of interesting functionalities for applications in the field of chemical and biological sensing.

In this work, we experimentally demonstrate a device platform for trapping and sensing of microparticles by

a)Author to whom correspondence should be addressed. Electronic mail: elelc@nus.edu.sg

exploiting the advantages provided by the microfluidics and metamaterials operating in the THz spectral region. The device consists of microfluidic channels integrated with trapping structures on top of a metamaterial structure to trap the microparticles in the most sensitive region of each unit cell, and the changes in the THz transmission response of the metamaterial are used to examine the type and quantity of the trapped microparticles.

II. DESIGN AND FABRICATION

The schematic of the proposed microfluidic metamaterial sensor (MMS) device for the selective trapping and sensing of microparticles is shown in Fig. 1(a). The split ring resonator (SRR) structure is selected as the metamaterial resonator. The incoming THz wave with electric field polarized in the direction parallel to the SRR gap excites the fundamental inductive-capacitive (LC) resonance of the SRR, where a circulating current in the metallic ring confines a strong electric field in the gap region. The LC resonance frequency of the SRR is determined by the inductance (L) of the square metal ring and capacitance (C) of the gap region using the expression, $f_r = 1/2\pi\sqrt{LC}$. Since C is a function of the permittivity, any changes in the dielectric property of the material positioned in the gap region will change its effective C, thereby resulting in a spectral shift of the LC resonance. The geometrical parameters of the SRR unit cell are shown in Fig. 1(b), where base length (L) = 30 μm, width (w) = 5 μm, and the capacitive gap (g) = 5 μm. In order to trap the microparticles at the capacitive gap of SRR geometry, a microfluidic system was integrated on top of the SRR structure. Quartz was selected as the substrate material to fabricate metallic resonator patterns as well as microfluidic structures because of its high transparency in the THz spectral region. SU-8 photoresist was chosen as the material for microfluidic structures for its capability of forming structures in microscale with a high aspect ratio. Moreover, the ultraviolet (UV) curable property of SU-8 allows easy and direct alignment of trapping structure fabrication on top of SRR patterns.

Among several presented trapping methods,[46] trapezoidal structures were utilized as the microfluidic trapping structures in this work. The simple design and fabrication process of trapezoidal trapping structures allow for the easier integration with the SRR below. In this design, microparticles can be trapped into the empty slots through the flow of liquid in between the two trapezoidal structures positioned at the capacitive gap of the SRR. However, once a particle is trapped, the flow resistance between the two trapezoids increases and as a result the subsequent liquid bypasses the trapped slot. This ensures that only one particle is trapped at the capacitive gap of each SRR, which is critical for quantitative estimation of microparticles being trapped. The metamaterial was designed by periodically arranging the SRR unit cells in a honeycomb structure, as shown in Fig. 1(c). This allows the liquid flow to carry subsequent particles into the next row of the empty trapping structures. The distance between two trapezoids was designed to be t = 5 μm to trap particles of larger size, in this case, aiming at polystyrene particles with a diameter of 20 μm suspended in isopropyl alcohol (IPA) solution.

Simulations were carried out using Computer Software Technology (CST) Microwave studio to study the effect of particle trapping on the resonance transmission response of the SRR metamaterial. The incoming THz pulse is illuminated on the SRR metamaterial at normal incidence with the electric component of the THz pulse being parallel to the SRR gap. The fundamental LC mode resonance of the planar SRR without trapping structures is designed at 1.04 THz, as shown in Fig. 2(a). When the SU-8 (with refractive index, n = 1.8) microfluidic structure is placed on the SRR, the LC resonance red shifts to 1.00 THz, due to the larger permittivity value of SU-8 compared to the air. Next, as IPA solution (n = 1.9) was added into the whole area covering the SRR with SU-8 trapping structures, the simulated LC resonance of the SRRs further red shifts to 0.85 THz, because of the higher refractive index of IPA. Finally, when a polystyrene particle (n = 1.6) with a diameter of 20 μm is trapped within the SU-8 trapping structure on top of the SRR gap region, the simulated LC resonance blue shifts to 0.87 THz. This is

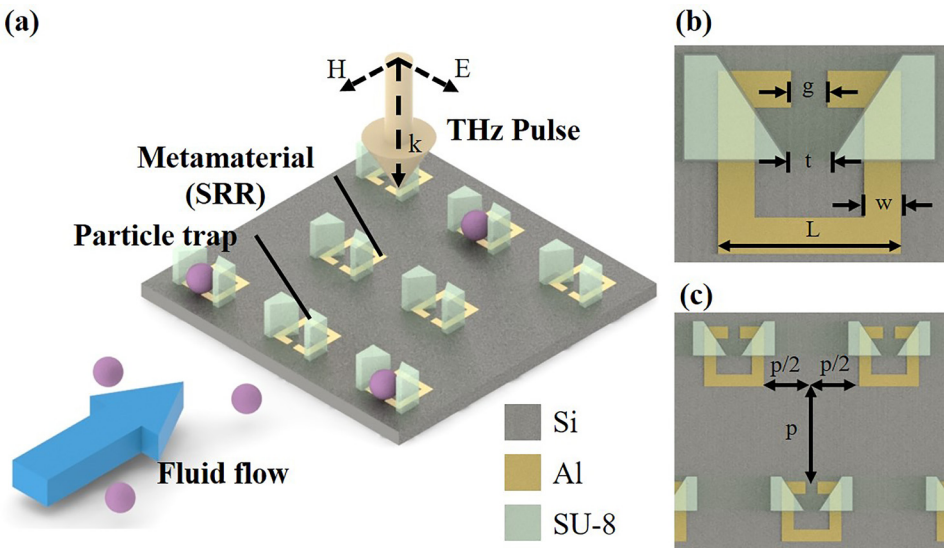

FIG. 1. (a) Schematic drawing of the proposed microfluidic metamaterial sensor (MMS) operating in the THz spectral region. (b) Geometrical parameters of the metamaterial unit cell along with the trapping structure (g = 5 μm, t = 5 μm, w = 5 μm, L = 30 μm) and (c) the corresponding metamaterial array design (p = 50 μm).

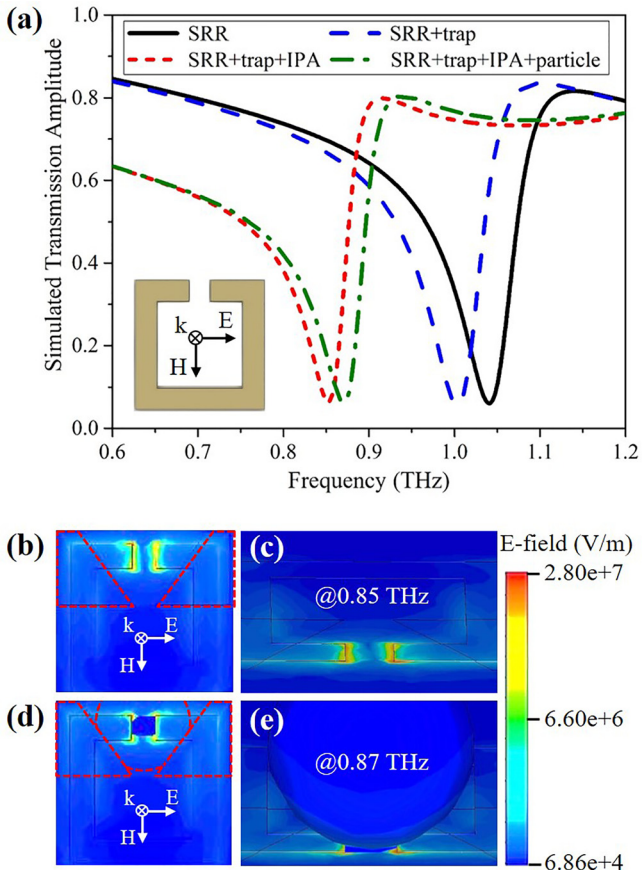

FIG. 2. (a) Simulated THz transmission spectrum for the SRR under the following conditions of only SRR, SRR with the trapping structure, SRR with the trapping structure plus IPA introduction, and SRR with the trapping structure plus IPA plus the polystyrene particle. (b) Top view and (c) perspective view of the simulated electric field distribution of the SRR in IPA at 0.85 THz when the particle is not trapped. (d) Top view and (e) perspective view of the simulated electric field distribution of SRR in IPA at 0.87 THz when the particle is trapped.

caused due to the lower refractive index of polystyrene with respect to IPA solution. The electric field distribution at the fundamental LC resonant frequency of the SRR was studied at various trapping configurations of the MMS. When no particle is trapped, there is a strong confinement of electric field in the capacitive gap region, as shown in Fig. 2(b). However, when the particle is trapped, the electric field in the gap region strongly couples to the particle, as shown in Fig. 2(d). This causes a spectral shift of the SRR LC mode resonance. Hence, based on the changes in the THz transmission spectral shift of LC resonance, the type of microparticle can be estimated.

Further simulations were carried out to determine the best particle trapping position on the SRR geometry to achieve the maximum sensitivity. By setting the center of the SRR gap region as the coordinate origin, the polystyrene particle along with its trapping structure was moved to different spatial positions along x- and y- directions on top of the SRR (Fig. 3(a)). The amount of resonance shift (Δf_r) was calculated as the difference between the initial resonance frequency of the SRR with trapping structures plus the IPA solution without the particle (0.85 THz) and with the particle trapped at various spatial positions. As shown in Fig. 3(b), the particle placed in the center of the gap region ($x = 0\,\mu m$, $y = 0\,\mu m$) results in the largest shift of LC resonance. The value of Δf_r decreases along the y-direction at any fixed x-position. This is due to the existence of stronger electric field strength at the SRR gap as shown in Fig. 2(b) and the strength fades out as the particle is displaced along the y-direction. In the case of particle being displaced along the x-direction (for $y = 0$), there is no significant change in the frequency shift Δf_r of the resonance. This observed distinctive variation in the values of the frequency shifts Δf_r along the x- or y-axis displacement of the particle is due to the anisotropic distribution of the confined electric field in the x- and y-directions. In other words, the electric field distribution along the x-direction is more uniform than its distribution along the y-direction in the SRR gap region.

The steps involved in the fabrication process for the demonstration of the MMS concept are shown pictorially in Fig. 4. The UV lithography process was first performed to structure the SRR patterns. Later, titanium (Ti) and aluminum (Al) metal of thickness 10 nm and 100 nm, respectively, were deposited using a thermal evaporation method followed by the lift-off process to obtain the desired metamaterial patterns (Fig. 4(a.1)). The trapping structure and the microfluidic channel of 25 μm height were aligned and patterned on top of each SRR gap using SU-8 photoresist (Fig. 4(a.2)). As a sealing material, a polyethylene terephthalate (PET) substrate of thickness 100 μm was used because of its high

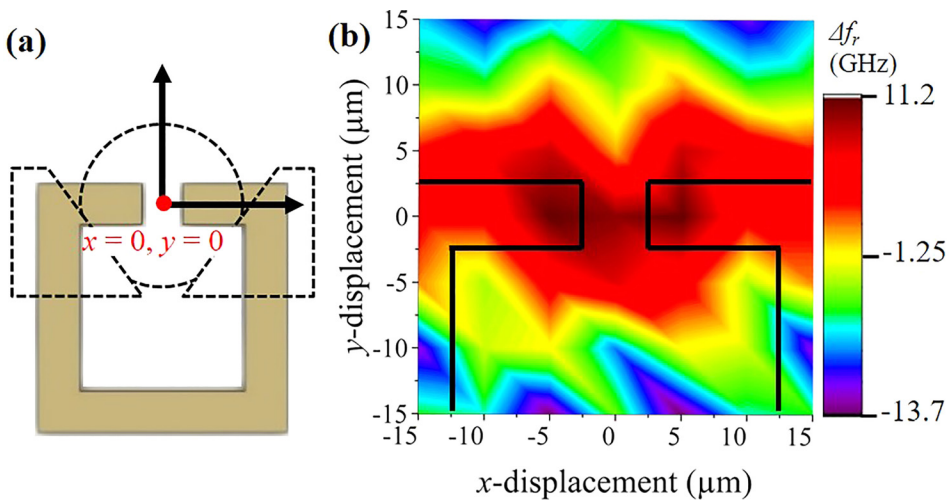

FIG. 3. (a) Schematic illustration of displacing the particle with the trapping structure from the center of SRR's gap. (b) Contour plot showing the resonant frequency shift when the particle is trapped at different positions (along *x* and *y* axes) with respect to the SRR gap (the black line indicates the edge of the SRR structure).

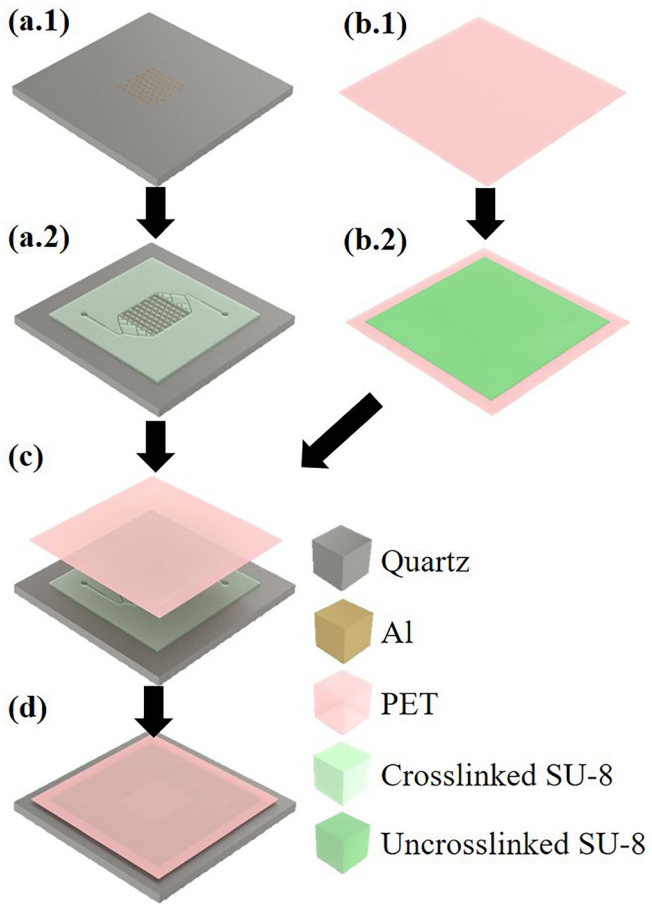

FIG. 4. Fabrication process of the proposed MMS device (a.1) Aluminum (Al) patterning of the SRR on the quartz substrate using a lift off process by Ultraviolet (UV) lithography and thermal evaporation. (a.2) Formation of a microfluidic channel and particle trapping using UV lithography of SU-8 photoresist. (b.1) Oxygen (O_2) plasma treatment of the polyethylene terephthalate (PET) substrate. (b.2) Spin coating the SU-8 photoresist on top of PET as an adhesive layer. (c) Bonding of the bottom quartz chip and the top layer. (d) UV exposure of the bonded chip to cure the adhesive SU-8 layer.

transparency in the THz and visible spectrum (Fig. 4(b.1)). It was treated by oxygen (O_2) plasma before spin-coating a 50 μm thick SU-8 as an adhesive layer (Fig. 4(b.2)). Subsequently, the PET with uncrosslinked SU-8 was flipped and bonded on top of the bottom SRR substrate with a SU-8 trapping structure chip (Fig. 4(c)). Finally, the bonded microfluidic chip was exposed to UV light to crosslink the adhesive SU-8 layer, thereby making a strong seal to prevent

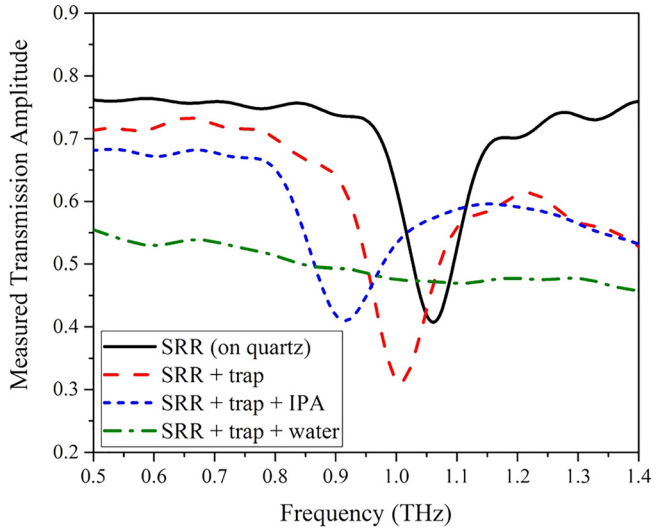

FIG. 6. Measured transmission spectra of liquid property measurement: SRR patterned on the quartz substrate (black solid line), SRR on quartz with the trapping structure (red dashed line), IPA (isopropyl alcohol) solution injected into the microfluidic channel (blue short dashed line), and DI water injected into the microfluidic channel (green dashed dotted line).

solution leakage during the measurements (Fig. 4(d)). Fig. 5(a) shows the photograph of the MMS device (1 cm × 1 cm) fabricated on a quartz substrate of dimension 4 cm × 4 cm. Fig. 5(b) depicts the microscopic image of the MMS active area, where the trapping structures positioned on top of each SRR with two trapezoidal structures are seen. Due to the limitations of the alignment system for the photolithography process, there is a slight misalignment of the trapping structure from the center of the SRR gap. In our fabrication, we observed $\Delta x = +4\,\mu m$ and $\Delta y = +5\,\mu m$ alignment error, respectively, along the horizontal and the vertical directions.

III. DEVICE CHARACTERIZATION

The THz response of the fabricated MMS device was characterized using a THz time domain spectroscopy (THz-TDS) system. The incoming THz wave was incident normally on the device with its electric field parallel to the gap of the SRR. The LC mode resonance frequency of the SRR on quartz substrate without the trapping structures was measured at 1.06 THz, as shown in Fig. 6. With the fabrication of the SU-8 trapping structure and the sealing layer, the

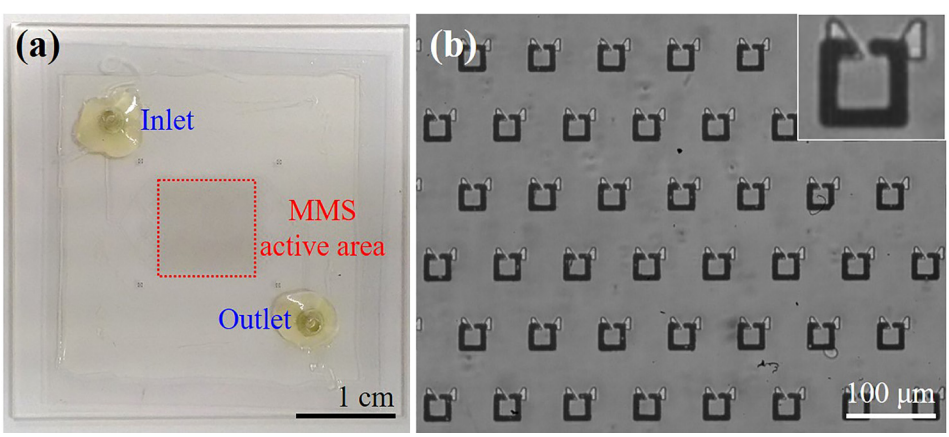

FIG. 5. (a) Photographic image of the fabricated MMS device on quartz showing the inlet and outlet ports of the microfluidic channel along with the MMS active area marked at the center. (b) Optical microscopic image of the trapezoidal traps on top showing SRR structures in the MMS active area.

measured LC resonance frequency red shifts to 1.00 THz, and shows good agreement with the simulated results. IPA and deionized (DI) water were injected into the fluidics channel without any microparticles. When DI water was injected into the channel, the amplitude of the transmitted THz signal was strongly modulated and there was no observable resonance dip in the measured spectrum. This is due to strong absorption of water in the THz frequencies. Alternatively, for IPA, the resonance is observed at 0.91 THz. The red shift in the measured resonance frequency is caused due to the increased refractive index of IPA relative to air. The integration of microfluidics channel structures and the metamaterial enables detection of refractive index of liquids using a small sample volume.

As a demonstration of particle trapping and detection, polystyrene beads (Phosphorex) with a diameter of 20 μm were used. After filling the channel with pure IPA, polystyrene beads suspended in IPA solution were injected using a syringe pump. From optical microscopic observation, 15% of the SRRs were occupied by beads in a random order. The transmission spectrum of the trapped beads in IPA solution was then measured and a resonance dip was observed at 0.92 THz, as shown in Fig. 7. The measured resonance frequency shift of 10 GHz was achieved for the MMS with and without polystyrene particles. The blue shift in the resonance is caused due to the lower refractive index of polystyrene with respect to IPA. The relatively small resonant shift in the measurements can be attributed to the alignment errors in the fabrication process and reduced number of particles trapped in the SRR gaps. Since the transmitted signal is a collective response of each meta-atom, the reduction in the number of SRRs with trapped particles also results in a decrease of resonance strength. Limitations such as the trapping rate and alignment error can be readily overcome by further optimization of resonator design, trapping structural design, robust fabrication process, and experimental conditions.

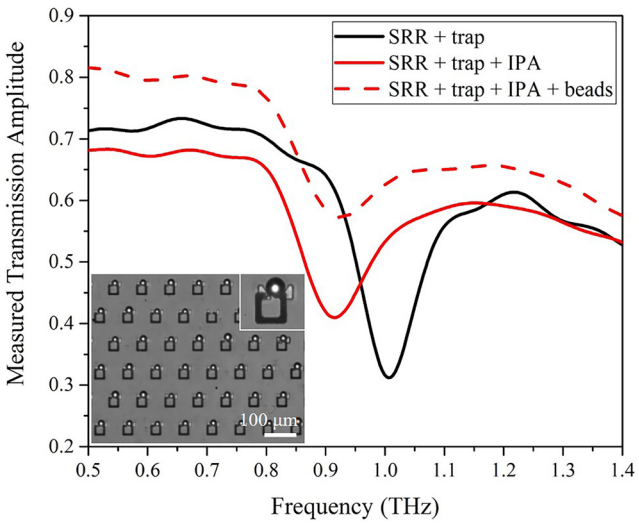

FIG. 7. Measured transmission spectra of the bead trapping experiment: SRR with trap (black solid line), SRR with trap in IPA solution (red solid line), and polystyrene beads trapped in IPA solution (red dashed line), and the inset figure depicts the optical microscopic image of polystyrene beads trapped by the SU-8 trapping structure at the gap of the SRR pattern.

Furthermore, the proposed MMS is an ideal platform for the live biological cell trapping and detection; however the limitation of water absorption should be addressed. This can be done by reducing the water volume in the trapping structures. Thus, the proposed MMS device concept allows for the label-free, non-destructive, and remote sensing of microparticles by taking advantage of the complementing features offered by the research fields of microfluidics, metamaterials, and terahertz spectroscopy.

IV. CONCLUSION

In summary, a platform for size selective trapping and sensing of microparticles is demonstrated by integrating microfluidics with metamaterials operating at terahertz frequencies. We designed and fabricated periodically spaced SRR structures on a quartz substrate consisting of SU-8/PET microfluidic channels to selectively trap the microparticles in the most sensitive gap region of the SRRs. Due to the predefined number of microparticles trapped in each SRR, the THz transmission response can provide both the qualitative and quantitative estimation of the trapped particles in terms of their resonance frequency and the amplitude modulation, respectively. The maximum blue shift of 10 GHz is achieved for 15% particle trapping rate. The versatility of metamaterial resonator designs along with the selective trapping functionality of microfluidics operating in the low energy THz spectral range will open up new research opportunities focused on label-free detection, biomolecular sensing and quantification of microparticles in the terahertz and infrared frequencies.

ACKNOWLEDGMENTS

K.S., P.P., C.P.H., and C.L. acknowledge the financial support from the research grant of ARF Tier2-MOE2012-T2-2-154; NRF-CRP15-2015-02 at the National University of Singapore, Singapore. National Natural Science Foundation of China under Grant No. 61474078 at NUS (Suzhou) Research Institute, Suzhou, China, and No. 61674104 at Shanghai Jiao Tong University, Shanghai, China. M.M. and R.S. acknowledge the research funding support from NTU startup Grant No. M4081282, Singapore MOE Grant Nos. M4011362, M4011534, MOE2011-T3-1-005, and MOE2015-T2-2-103.

[1]B. Ferguson and X.-C. Zhang, "Materials for terahertz science and technology," Nat. Mater. **1**, 26 (2002).
[2]N. I. Zheludev and Y. S. Kivshar, "From metamaterials to metadevices," Nat. Mater. **11**, 917 (2012).
[3]R. A. Shelby, D. R. Smith, and S. Schultz, "Experimental verification of a negative index of refraction," Science **292**, 77 (2001).
[4]J. Valentine, S. Zhang, T. Zentgraf, E. Ulin-Avila, D. A. Genov, G. Bartal, and X. Zhang, "Three-dimensional optical metamaterial with negative refractive index," Nature **455**, 376 (2008).
[5]H. Tao, N. I. Landy, C. M. Bingham, Z. Zhang, R. D. Averitt, and W. J. Padilla, "A metamaterial absorber for the terahertz regime: Design, fabrication and characterization," Opt. Express **16**, 7181 (2008).
[6]N. I. Landy, S. Sajuyigbe, J. J. Mock, D. R. Smith, and W. J. Padilla, "Perfect metamaterial absorber," Phys. Rev. Lett. **100**, 207402 (2008).
[7]N. Fang, H. Lee, C. Sun, and X. Zhang, "Sub-diffraction-limited optical imaging with a silver superlens," Science **308**, 534 (2005).

[8]P. Pitchappa, M. Manjappa, C. P. Ho, R. Singh, N. Singh, and C. Lee, "Active control of electromagnetically induced transparency analog in terahertz MEMS metamaterial," Adv. Opt. Mater. **4**, 541 (2016).
[9]C. P. Ho, P. Pitchappa, and C. Lee, "Digitally reconfigurable binary coded terahertz metamaterial with output analogous to NOR and AND," J. Appl. Phys. **119**, 153104 (2016).
[10]D. Hasan, C. P. Ho, and C. Lee, "Thermally tunable absorption-induced transparency by a quasi 3D bow-tie nanostructure for nonplasmonic and volumetric refractive index sensing at mid-IR," Adv. Opt. Mater. **4**, 943 (2016).
[11]D. Schurig, J. J. Mock, B. J. Justice, S. A. Cummer, J. B. Pendry, A. F. Starr, and D. R. Smith, "Metamaterial electromagnetic cloak at microwave frequencies," Science **314**, 977 (2006).
[12]F. Ma, Y.-S. Lin, X. Zhang, and C. Lee, "Tunable multiband terahertz metamaterials using a reconfigurable electric split-ring resonator array," Light: Sci. Appl. **3**, e171 (2014).
[13]P. Pitchappa, C. P. Ho, L. Dhakar, Y. Qian, N. Singh, and C. Lee, "Periodic array of subwavelength MEMS cantilevers for dynamic manipulation of terahertz waves," J. Microelectromech. Syst. **24**, 525 (2015).
[14]P. Pitchappa, C. P. Ho, Y. Qian, L. Dhakar, N. Singh, and C. Lee, "Microelectromechanically tunable multiband metamaterial with preserved isotropy," Sci. Rep. **5**, 11678 (2015).
[15]P. Pitchappa, C. P. Ho, L. Dhakar, Y. Qian, and C. Lee, "Microelectromechanically reconfigurable interpixelated metamaterial for independent tuning of multiple resonances at terahertz spectral region," Optica **2**, 571 (2015).
[16]Y.-S. Lin and C. Lee, "Tuning characteristics of mirrorlike T-shape terahertz metamaterial using out-of-plane actuated cantilevers," Appl. Phys. Lett. **104**, 251914 (2014).
[17]P. Pitchappa, C. P. Ho, L. Cong, R. Singh, N. Singh, and C. Lee, "Reconfigurable digital metamaterial for dynamic switching of terahertz anisotropy," Adv. Opt. Mater. **4**, 391 (2016).
[18]P. Pitchappa, M. Manjappa, C. P. Ho, R. Singh, N. Singh, and C. Lee, "Active control of electromagnetically induced transparency with dual dark mode exciatation pathway using MEMS based tri-atomic metamolecules," Appl. Phys. Lett. **109**, 211103 (2016).
[19]T. Chen, S. Li, and H. Sun, "Metamaterials application in sensing," Sensors **12**, 2742 (2012).
[20]M. Tonouchi, "Cutting-edge terahertz technology," Nat. Photonics **1**, 97 (2007).
[21]R. M. Woodward, B. E. Cole, V. P. Wallace, R. J. Pye, D. D. Arnone, E. H. Linfield, and M. Pepper, "Terahertz pulse imaging in reflection geometry of human skin cancer and skin tissue," Phys. Med. Biol. **47**, 3853 (2002).
[22]H. B. Liu, G. Plopper, Y. Chen, B. Ferguson, and Z.-C. Zhang, "Sensing minute changes in biological cell monolayers with THz differential time-domain spectroscopy," Biosens. Bioelectron. **22**, 1075 (2007).
[23]A. Menikh, R. MacColl, C. A. Mannella, and X.-C. Zhang, "Theahertz biosensing technology: Frontiers and progress," ChemPhysChem **3**, 655 (2002).
[24]C. Seco-Martorell, V. Lopez-Dominguez, G. Arauz-Garofalo, A. Redo-Sanchez, J. Palacios, and J. Tejada, "Goya's artwork imaging with Terahertz waves," Opt. Express **21**, 17800 (2013).
[25]S. J. Park, J. T. Hong, S. J. Choi, H. S. Kim, W. K. Park, S. T. Han, J. Y. Park, S. Lee, D. S. Kim, and Y. H. Ahn, "Detection of microorganisms using terahertz metamaterials," Sci. Rep. **4**, 4988 (2014).
[26]S. J. Park, B. H. Son, S. J. Choi, H. S. Kim, and Y. H. Ahn, "Sensitive detection of yeast using terahertz slot antennas," Opt. Express **22**, 30467 (2014).
[27]S. J. Park, S. W. Jun, A. R. Kim, and Y. H. Ahn, "Terahertz metamaterial sensing on polystyrene microbeads: Shape dependence," Opt. Mater. Express **5**, 2150 (2015).
[28]J. F. O'Hara, R. Singh, I. Brener, E. Smirnova, J. Han, A. J. Taylor, and W. Zhang, "Thin-film sensing with planar terahertz metamaterials: Sensitivity and limitations," Opt. Express **16**, 1786 (2008).
[29]R. Singh, W. Cao, I. Al-Naib, L. Cong, W. Withayachumnankul, and W. Zhang, "Ultrasensitive terahertz sensing with high-Q Fano resonances in metasurfaces," Appl. Phys. Lett. **105**, 171101 (2014).
[30]L. Cong, S. Tan, R. Yahiaoui, F. Yan, W. Zhang, and R. Singh, "Experimental demonstration of ultrasensitive sensing with terahertz metamaterial absorbers: A comparison with the metasurfaces," Appl. Phys. Lett. **106**, 031107 (2015).
[31]D.-K. Lee, J.-H. Kang, J.-S. Lee, H.-S. Kim, C. Kim, J. H. Kim, T. Lee, J.-H. Son, Q-H. Park, and M. Seo, "Highly sensitive and selective sugar detection by terahertz nano-antennas," Sci. Rep. **5**, 15459 (2015).
[32]O. Limaj, D. Etezadi, N. J. Wittenberg, D. Rodrigo, D. Yoo, S.-H. Oh, and H. Altug, "Infrared plasmonic biosensor for real-time and label-free monitoring of lipid membranes," Nano Lett. **16**, 1502 (2016).
[33]A. Berrier, M. C. Schaafsma, G. Nonglaton, J. Bergquist, and J. G. Rivas, "Selective detection of bacterial layers with terahertz plasmonic antennas," Biomed. Opt. Express **3**, 2937 (2012).
[34]W. Withayachumnankul, H. Lin, K. Serita, C. M. Shah, S. Sriram, M. Bhaskaran, M. Tonouchi, C. Fumeaux, and D. Abbott, "Sub-diffraction thin-film sensing with planar terahertz metamaterials," Opt. Express **20**, 3345 (2012).
[35]W. Withayachumnankul, K. Jaruwongrungsee, A. Tuantranont, C. Fumeaux, and D. Abbott, "Metamaterial-based microfluidic sensor for dielectric characterization," Sens. Actuators, A **189**, 233 (2013).
[36]A. Ebrahimi, W. Withayachumnankul, S. Al-Sarawi, and D. Abbott, "High-sensitivity metamaterial-inspired sensor for microfluidic dielectric characterization," IEEE Sens. J. **14**, 1345 (2014).
[37]G. M. Whitesides, "The origins and the future of microfluidics," Nature **442**, 368 (2006).
[38]L. Y. Yeo, H.-C. Chang, P. P. Y. Chan, and J. R. Friend, "Microfluidic devices for bioapplications," Small **7**, 12 (2011).
[39]J. El-Ali, P. K. Sorger, and K. F. Jensen, "Cells on chip," Nature **442**, 403 (2006).
[40]R. Sista, Z. Hua, P. Thwar, A. Sudarsan, V. Srinivasan, A. Eckhardt, M. Pollack, and V. Pamula, "Development of a digital microfluidic platform for point of care testing," Lab Chip **8**, 2091 (2008).
[41]H. Wang, C.-H. Chen, Z. Xiang, M. Wang, and C. Lee, "Convection-driven long-range linear gradient generator with dynamic controls," Lab Chip **15**, 1445 (2015).
[42]X. Fan, I. M. White, S. I. Shopova, H. Zhu, J. D. Suter, and Y. Sun, "Sensitive optical biosensors for unlabeled targets: A review," Anal. Chem. Acta **620**, 8 (2008).
[43]K. K. Zeming, S. Ranjan, and Y. Zhang, "Rotational separation of non-spherical bioparticles using I-shaped pillar arrays in a microfluidic device," Nat. Commun. **4**, 1625 (2013).
[44]M. E. Warkiani, G. Guan, K. B. Luan, W. C. Lee, A. A. S. Bhagat, P. K. Chaudhuri, D. S.-W. Tan, W. T. Lim, S. C. Lee, P. C. Y. Chen, C. T. Lim, and J. Han, "Slanted spiral microfluidics for the ultar-fast, label-free isolation of circulating tumor cells," Lab Chip **14**, 128 (2014).
[45]D. Di Carlo, L. Y. Wu, and L. P. Lee, "Dynamic single cell culture array," Lab Chip **6**, 1445 (2006).
[46]X. Xhu, P. Sarder, Z. Li, and A. Nehorai, "Optimization of microfluidic microsphere-trap arrays," Biomicrofluidics **7**, 014112 (2013).
[47]J. Kim, J. Erath, A. Rodriguez, and C. Yang, "A high-efficiency microfluidic device for size-selective trapping and sorting," Lab Chip **14**, 2480 (2014).
[48]H. Chen, J. Sun, E. Wolvetang, and J. Cooper-White, "High-throughput, deterministic single cell trapping and long-term clonal cell culture in microfluidic devices," Lab Chip **15**, 1072 (2015).